



TURBOMACHINERY & PUMP SYMPOSIA | HOUSTON, TX
SEPTEMBER 13-15, 2022
SHORT COURSES: SEPTEMBER 12, 2022

MEASUREMENT AND CALCULATION OF A SELF-EQUALIZED TILTING-PAD THRUST BEARING UNDER STATIC MISALIGNMENT

Nico Havlik
Product Manager
RENK Group
Hannover, Germany

Philipp Sebastian Winking
Research Associate
Clausthal University of Technology
Clausthal-Zellerfeld, Germany

Kai Lindloff
Research Engineer
RENK Group
Hannover, Germany

Christian Kraft
Research Associate
Clausthal University of Technology
Clausthal-Zellerfeld, Germany

Prof. Dr. Hubert Schwarze
Head of Institute for Tribology
and Energy Conversion Machinery
Clausthal University of Technology
Clausthal-Zellerfeld, Germany



Nico Havlik is lead engineer and business development manager for Turbomachinery bearings at RENK Group in Hannover, Germany. Since 2017, he worked in different departments and has many experiences in vertical and horizontal bearing applications. Previously to RENK, he worked nine years as R&D engineer at MAN-Energy Solutions in Berlin. He is speaker at Association of German Engineers (VDI) on fluid film bearings and its influence on rotordynamic behaviour. He authored and co-authored a few papers and owns a patent.



Philipp Winking is research associate at the Institute of Tribology and Energy Conversion Machinery (ITR) of Clausthal University of Technology. Since 2017 he designed and build-up a test-rig for vertically arranged fluid film bearings, on which he performed various experimental investigations for the industry. His focus in particular includes the design of test-rigs, simulation and experiment of hydrodynamic thrust and journal bearings, rotordynamics, hydraulics as well as sensors and electronics. He co-authored a paper regarding the transient run-up of journal bearings and owns a patent.



Kai Lindloff is research engineer at RENK Group in Hannover, Germany. He received his diploma in mechanical engineering from Technical University of Braunschweig, where he worked as a research associate from 1992 to 1999 and performed experimental investigations on hydrodynamic thrust bearings and on rotordynamics of journal bearings. Since 2000, he is working for RENK, planning and performing test campaigns on horizontal and vertical bearings, software programming the RENK calculation tools and performing various bearing calculations.



Christian Kraft is research associate at the Institute of Tribology and Energy Conversion Machinery (ITR) of Clausthal University of Technology. The simulation of fluid film bearings and the development of tools for the calculation of fluid bearings are his main tasks. He is the developer of the thrust bearing calculation program COMBROS-A. Since 2008 he continuously further developed COMBROS-A at University of Clausthal, while he authored and co-authored several papers.



Hubert Schwarze is head of the Institute of Tribology and Energy Conversion Machinery (ITR) at Clausthal University of Technology since 2000. Previously, he worked for 8 years at Federal Mogul as design manager and technical director. The focus of his work is tribology, rheology, high-speed plain bearings, rolling bearings and rotor dynamics. The institute focuses on high-speed axial and radial plain bearings in theory and experiment.

ABSTRACT

Tilting-pad thrust bearings which include a self-equalizing feature, ensure reliable and safe operation especially under conditions on which misalignment between bearing and collar occurs. One common method to incorporate such a self-equalizing feature to a thrust tilting-pad bearing is the usage of leveling links. Radii and spherical contacts ensure a free rolling surface between the links, thrust pads and bearing housing. However, the verification whether a design works properly can be relatively challenging. For example, the friction forces between all the radii contacts always lead to different residual misalignments between the pads. This leads to a periodic rotational distribution of the hydrodynamic pressure and thus to different temperatures of each pad.

This paper shows detailed measurements of a self-equalizing thrust tilting-pad bearing using leveling links. The test campaign includes a wide range of bearing to collar misalignment and operating conditions. The measurements show, that such a mechanical equalizing-mechanism may sufficiently balance very large deflections, despite the fact, that the residual pad misalignment of each pad due to friction lead to a relative high temperature difference between the pads.

Furthermore, the paper presents a methodology of calculating the bearing behavior of self-equalizing thrust bearings to generate a better understanding and assessment of the proper function of such a bearing design. It presents the development of a mechanical model, which can iteratively solve a FEA software and a thermo-elastic-hydrodynamic (TEHD) software for fluid-film bearings.

INTRODUCTION

High-speed turbomachinery applications such as compressors and gas or steam turbines normally use fluid film bearings lubricated by oil to ensure reliable and safe operation. Those fluid film bearings build-up an oil film pressure which separates shaft and bearing surfaces. However, this distance or oil film thickness is relatively small and requires elaborate equipment to tolerate bearing to collar misalignment in addition to the manufacturing tolerances. The estimation of such elastic deformation requires for example very time-consuming FEA simulations and tolerance analysis. In addition, accurate load calculation resulting from the aerodynamic forces of the turbomachinery process is required as well.

As a result of such bearing to collar misalignment, the thrust load distribution between the different thrust pads will change and become more uneven. Hence, the hydrodynamic oil film pressure and thus the respective temperatures will increase at some thrust pads. Furthermore, higher hot spot temperatures will occur while power losses increases and oil lifetime decreases. In some cases, this could lead to serious machine damage.

Another approach is the compensation of the bearing to collar misalignment, shaft bending and related elastic deformation by using a self-equalizing tilting-pad thrust bearing. These bearings include a mechanism to equalize the acting forces between the different tilting-pads and thus equalize the distance between each pad and the shaft.

This paper presents a common equalized tilting pad thrust bearing design, which obtains different leveling links between the thrust pads and bearing housing to compensate the misalignment. However, the sliding and rolling of the different contacts generate friction forces. Those forces reduce the equalization effect and lead to residual pad misalignment between the different thrust pads. Thus, different values of the fluid film thickness, oil film pressure and temperatures occur. This paper therefore includes measurements of those values within a wide range of loads, speeds and under different bearing to collar misalignments and also compares it with results of the bearing calculation software COMBROS-A. COMBROS-A (Schwarze and Kraft, 2013) is a thermo-elastic hydrodynamic software for fluid film bearings and available within the German Association for Drive Technology (FVA) and the Research Association for Internal Combustion Engines (FVV). To measure the bearing behavior, the test-rig for high speed and highly loaded thrust bearings at Institute of Tribology and Energy Conversion Machines (ITR) of University of Clausthal was used.

Measurements of thrust bearings under static bearing to collar misalignment are limited. In 1985, Gardner presented laboratory tests of two different designs of a self-equalized tilting pad thrust bearing. One was carried out according to the standard design of that time and another included design changes to reduce the friction between the leveling links. He measured the overturning moment for several collar to bearing misalignments up to 0.35° and showed that within both designs a different friction was generated. He additionally showed that the temperature level of the friction-optimized design could be reduced. The measured pad temperatures were presented at the common position of 75 %-75 % described within API 670 and result from the average temperature of all incorporated tilting pads. However, the paper does not provide details, like the periodic course of each pad temperature in direction of rotation, to understand how the friction between the leveling links affects the equalizing mechanism or residual pad misalignment of each pad. Glavatskih (2002) presented some measurements of a thrust bearing under misalignment. Despite the equalization system, he also recognized differences in the oil film pressure of each pad. However, he does not include details to this fact. Schwarze and Kraft (2013) include a wide range of thrust bearings and measurements to present the validation of COMBROS-A. They presented a validation of a tapered-land thrust bearing under bearing to collar misalignment. This example includes a periodic course of the pad temperatures, this means it shows a continuous rise of the measured pad temperature in circumferential direction starting from the pad

with the lowest pad temperature to the pad temperature of next pad and so on up to the pad temperature of the pad with the highest pad temperature. Within this validation, the author iterated the misalignment until he received the best match on the value and periodic course of the measured and calculated temperature, which results at a misalignment of 0.0002 in (or $0,005\text{ mm}$). However, additional measuring parameters like oil film thickness and oil film pressure do not match with the calculation under misalignment between bearing and collar. The authors relate this on the one hand to the simplified thermo-elastic hydrodynamic (TEHD) effects considered within the approximate calculation model and on the other hand to the quality measurements of the geometry, which may have the same range as the measurement uncertainties. Recently, Koosha and San Andrés (2020) developed a calculation model to predict self-equalized tilting pad thrust bearings. This calculation tool includes the pad's self-equalizing mechanism (of the exact geometry of the leveling links and the friction acting between the leveling links and the tilting pad or housing) and an earlier TEHD analysis tool, which was widely validated. The presented example includes predictions of a thrust bearing operating at $4,000\text{ rpm}$ and a specific pad thrust load ranging from about $73\text{ to }508\text{ psi}$ (or $0.5\text{ to }3.5\text{ MPa}$) and a static misalignment between bearing and collar of 0.01° . However, compared to the common operating conditions of such self-equalized tilting pad thrust bearings, the shown static misalignment of 0.01° and the speed range is relatively low and a validation of the results difficult to implement in practice.

This paper therefore presents additional experiments on a self-equalized tilting pad thrust bearing under static bearing to collar misalignment. It includes a turning speed ranging up to $18,000\text{ rpm}$ and a static bearing to collar misalignment up to 0.41° . It points out the residual pad misalignment at different loads and speeds and provides a methodology to consider the self-equalizing feature during the design phase. It additionally presents a validation of the predictive software on the misalignment functionality and the development of a mechanical model, which iterates a FEA software and the TEHD-software COMBROS-A even under a relatively high static misalignment between bearing and collar of 0.41° . With this model, the remaining friction forces from the different contacts and thus the residual pad misalignment can be predicted. As a result, the bearing behavior of a self-equalizing thrust bearing can be better understood and assessed.

BEARING DESIGN

The fundamental design of a customized self-equalizing bearing is relatively complex and requires a deep understanding in the functionality of fluid film bearings, design limitations and tolerances. Especially the limitation in available space at the test-rig described below required some sophisticated design changes. Nevertheless, the final design is very similar to the common standard series of self-equalizing thrust tilting-pad bearings. **Figure 1** shows the customized self-equalizing design. Please note, the test-rig includes a vertical shaft orientation. **Table 1** includes the most important bearing parameters. **Table 2** shows the name and position number of the relevant parts. The relatively small and constant amount of available oil flow results from limitations of the test-rig's oil system, while the design of the test-rig originally considered tests of flooded bearings only. However, this does not affect the validation since the calculation will include the same amount of oil.

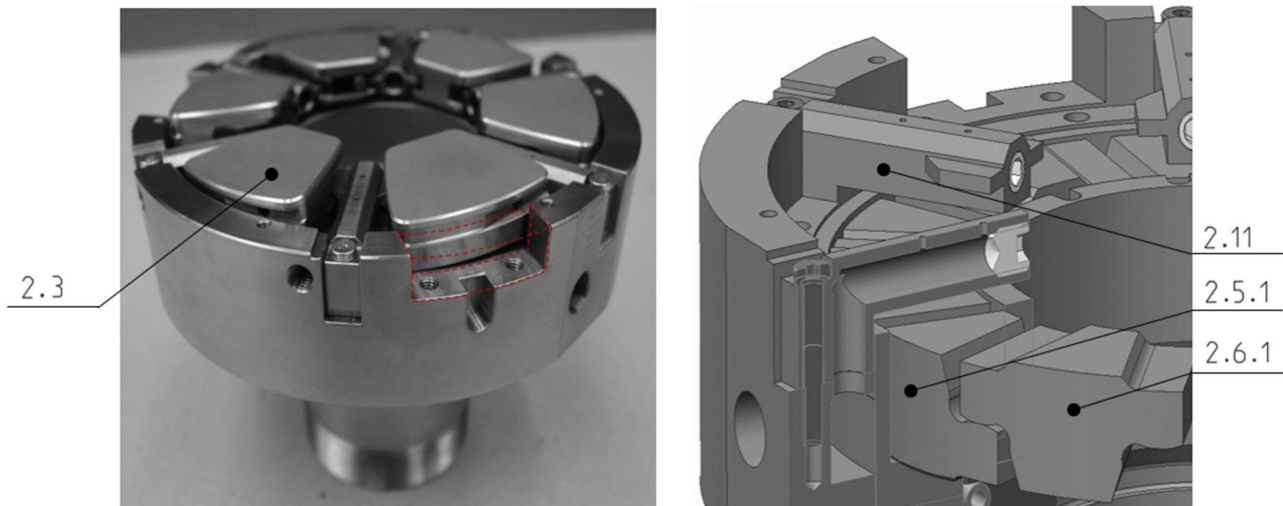


Figure 1 Self-equalizing thrust tilting-pad bearing for test-rig campaign

Table 1 Thrust bearing parameter

• Inner axial bearing diameter:	$D_i \approx 2.13''$	(54 mm)
• Outer axial bearing diameter:	$D_o \approx 4.65''$	(118 mm)
• Thrust pad quantity:	$Z_{ax} = 6$	
• Oil flow:	$Q_{ax} \approx 3.6\text{ gpm}$	(13,5 l/min)

Assembly

The test bearing includes several features to enable a wide range of the test-rig capabilities. Due to the limited oil flow, the selected features provide optimal temperature behaviour of the bearing. **Figure 2** shows the main features and interface dimension of the test-rig bearing.

Table 2 Part names and position numbers

- Pos. 2.1 Housing
- Pos. 2.2 Support ring
- Pos. 2.3 Thrust tilting pad
- Pos. 2.3.1 Pock
- Pos. 2.5.1 Lower leveling link
- Pos. 2.6.1 Upper leveling link
- Pos. 2.11 Spray bar
- Pos. 2.12 Retention screw
- Pos. 2.13 Orifice
- Pos. 9 Seal

To reduce hot oil carry over efficiently, the design includes a directed lubrication technology and is therefore non-flooded. Position 2.11 shows the related spray bar and its retention screw 2.12, which provides an exchangeable orifice 2.13 to adjust the oil supply from flowing from the circumferential oil groove to the pocket. The spray bar additionally prevents the pad from falling out during assembly. The gap seal of position 9 throttles the inner side flow from the thrust bearing to the gap between the inner housing diameter and shaft and thus reduces the splashing losses within that gap. Please note, the installed gap seal (position 9) limits the inner side flow and may affect its temperature. Position 2.6.1 shows the upper leveling link, Position 2.5.1 the lower leveling link. Position 2.2 shows the support ring, which carries the leveling links and additionally provides a free pad mobility. The thrust tilting-pads 2.3 have an asymmetrical pivot ratio in direction of rotation of 60 % and a radial pivot ratio of 50 % and include a spherical pivot, see position 2.3.1. The design includes a rounded leading edge to ensure optimal incident flow and thus to provide optimal compromise on power losses and load carrying capacity. The rectangular milling grooves at the outer diameter of the housing, shown in **Figure 1** (left) as red broken line, serve to connect measurement transmitters and are closed by the transmitter after the assembly.

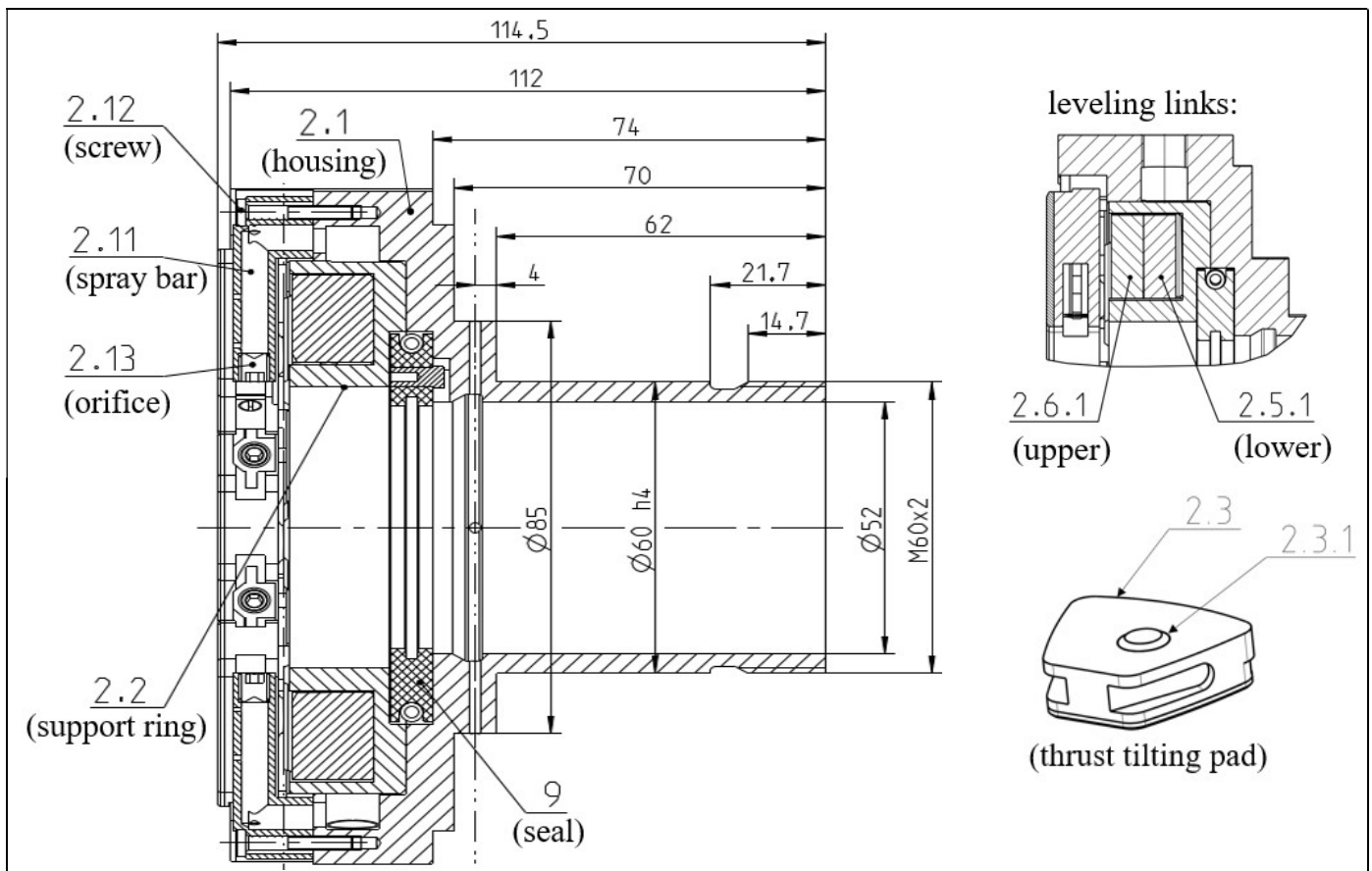


Figure 2 Test-rig bearing: Interface dimensions [mm] and specific features

Misalignment

To provide a specific and well-defined misalignment between bearing and thrust collar, the bearing's support ring (position 2.2) includes a machined misalignment Δy , see **Figure 3**. In total, four support rings V1 to V4 with different misalignments exist to investigate the influence of bearing to collar misalignment of the self-equalized tilting pad thrust bearing. **Table 3** shows the measured difference on the support ring thickness in relation to the outer axial diameter D_o .

V1 is the 'reference' support ring and includes almost no misalignment. Ring V2 and V3 include a typical bearing to collar misalignment according to the specific application in the field. Ring V4 includes an increased incorporated misalignment to cover all applications and maximum cases. The right figure shows the pad arrangement from pad I. to pad VI. The course of the machined misalignment of support ring 2.2 is manufactured in a way that the maximum wall thickness of 2.2 is below pad I and the minimum wall thickness is below pad IV. This means pad I. will generate the highest pad loading due to bearing misalignment and show the highest maximum pad temperature of all pads. **Table 3** shows the angle of the manufactured misalignment below pad I. and pad IV. Thus the rotational axis of the misalignment is shown in the right figure of **Figure 3** as red dotted line.

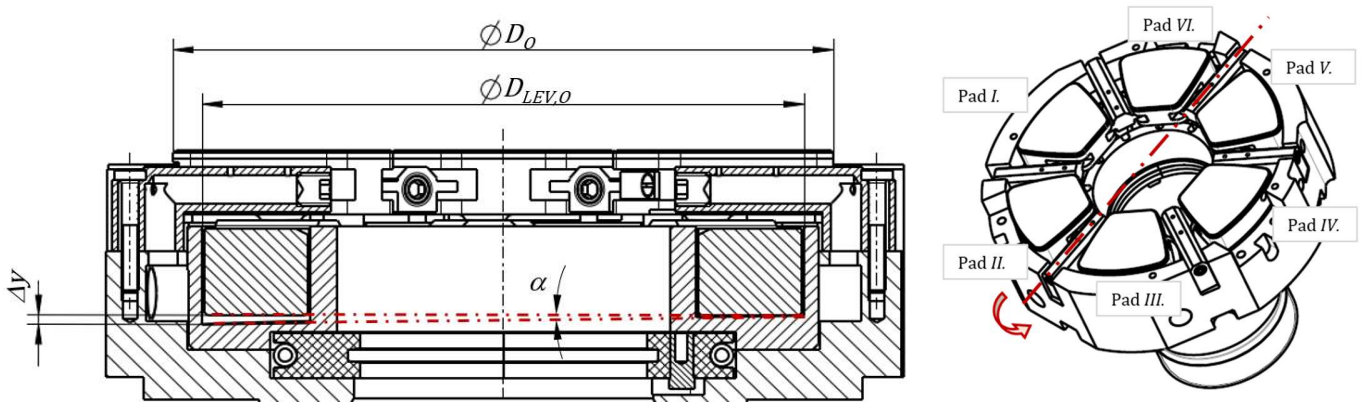


Figure 3 Visualization of the support ring and incorporated height difference Δy

Table 3 Thrust bearing's machined misalignment support ring

support ring	α	Δy
V1	0.005°	0.000394" (0,010 mm)
V2	0.095°	0.007677" (0,195 mm)
V3	0.188°	0.015197" (0,386 mm)
V4	0.412°	0.033386" (0,848 mm)

Where;

- D_o = outer axial diameter, in *inch* (*mm*)
- $D_{LEV,O}$ = outer diameter of leveling links, in *inch* (*mm*)
- Δy = height difference at the outer axial diameter, in *inch* (*mm*)
- α = angle of bearing to collar misalignment resulting from the manufactured height difference Δy , in °

NUMERICAL MODEL

Bearing Performance Calculation

This paper provides all results based on bearing performance calculations according to Schwarze and Kraft (2013). The software calculates thermo-elastic hydrodynamic deformations (TEHD) by iteratively solving the Reynolds and energy equation. It considers the gap geometry and oil film pressure within a 2-dimension field. The resulting minimum oil film thickness primary defines the load capacity. The temperature distribution of the oil, pad and shaft collar result from an estimation. The software obtains additional key features, such as:

- 3-dimensional field for the velocity (ϕ, r, z), temperature, viscosity and density
- effect of centrifugal forces
- approximation of thermal and mechanical deformation on thrust pads and shaft collar
- local laminar and turbulent flow transition
- cavitation at the divergent oil gap based on Elrod (1981)

Figure 4 shows the oil mixture model within the pockets between the thrust pads based on Heshmat and Pinkus (1986). It uses an “oil refreshing factor” f_r to describe the amount and temperature of the following pad’s oil inlet flow \dot{Q}_A .

The bearing calculation software handles the oil flow and its temperature from the previous pad of index A and of index E for the next pad as 2-dimensional fields (r, z) . It includes an estimation to evaluate the 3-dimensional temperature field (ϕ, r, z) and the oil heating.

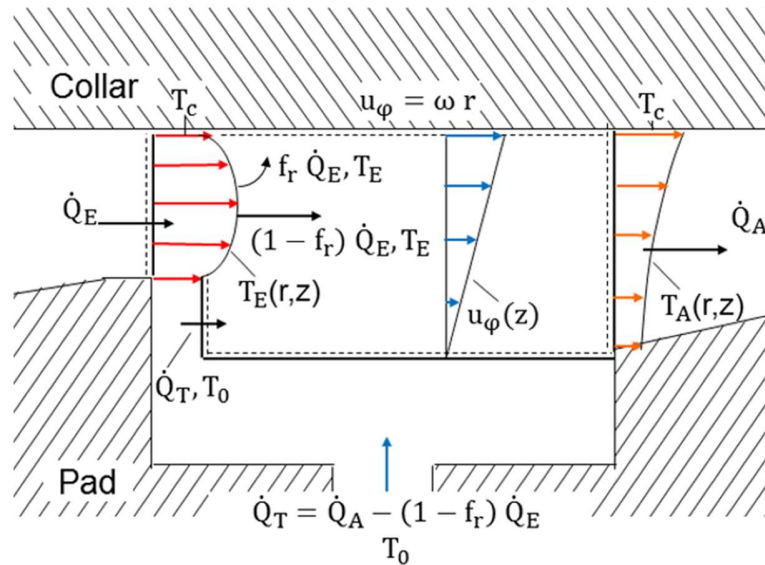


Figure 4 Oil mixture in the pocket (Heshmat and Pinkus, 1986)

Where:

- T_0 = oil supply temperature, in $^{\circ}F$ ($^{\circ}C$)
- \dot{Q}_T = oil supply flow to the pocket at T_0 , in gpm (l/min)
- T_E = oil temperature from previous thrust pad at trailing edge, in $^{\circ}F$ ($^{\circ}C$)
- \dot{Q}_E = oil inlet flow to the pocket from previous thrust pad at T_E , in gpm (l/min)
- T_A = oil inlet temperature to following thrust pad at the leading edge, in $^{\circ}F$ ($^{\circ}C$)
- \dot{Q}_A = oil supply flow to following thrust pad at T_A , in gpm (l/min)

TEST-RIG

For the experimental investigations, **Figure 5** shows high speed test-rig for fluid film thrust bearings, which was used.

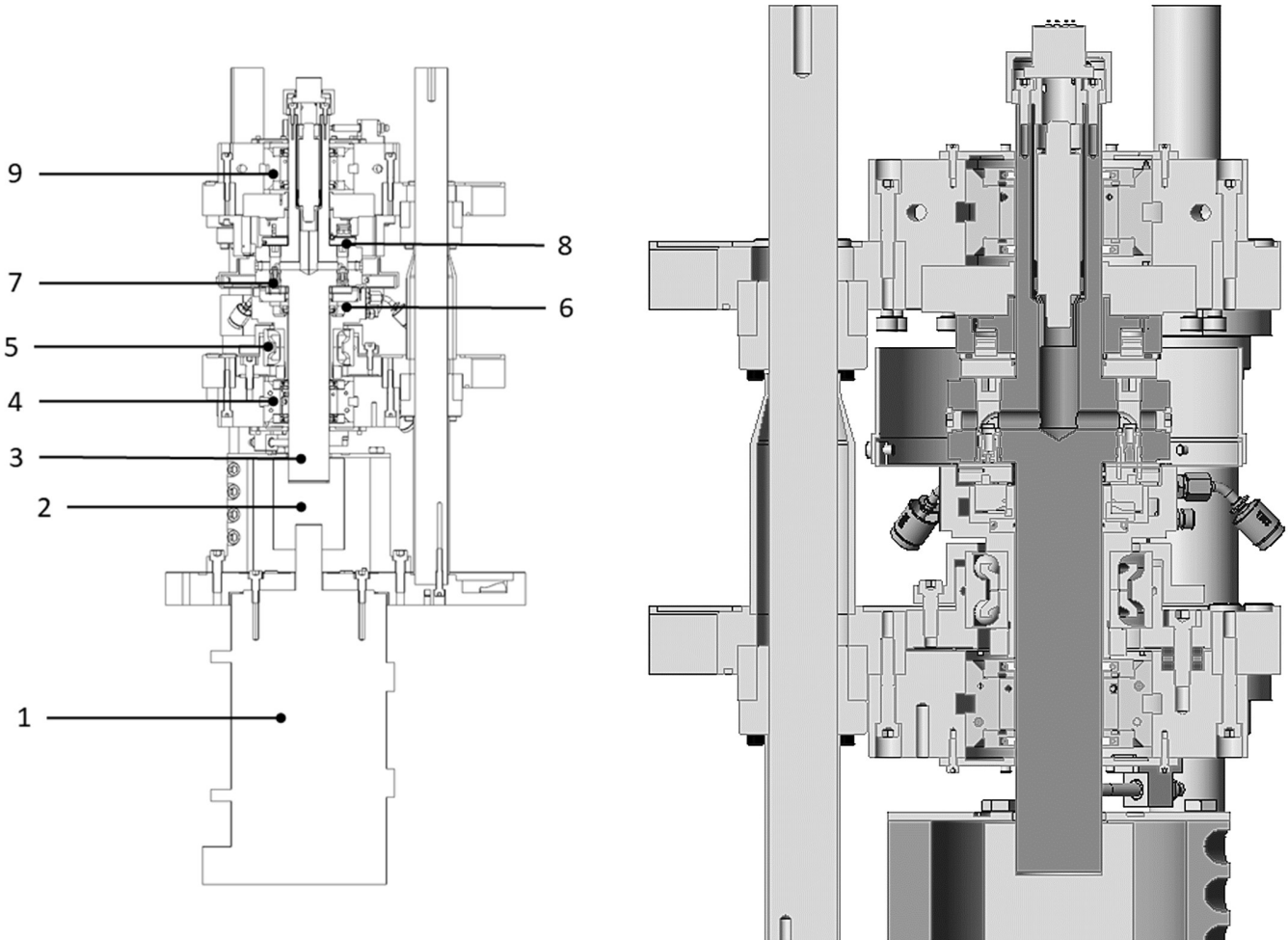


Figure 5 Axial bearing test-rig (left side: entire test-rig, right side: detailed test-bearing)

Position 1 shows the 46.9 *hp* (35 *kW*) electric drive located underneath the test set-up. Position 2 shows the angular and axial flexible coupling, which transmits the drive power to the shaft. Two hydrodynamic journal bearings (position 4 and 9) guide the vertical oriented shaft (position 3). Position 6 shows the tested self-equalization thrust tilting-pad bearing. The test-rig also includes an additional journal roller bearing (position 5) to avoid tilting of the test bearing and especially to measure the friction torque by using a strain gauge.

A load cylinder pushes the reverse acting hydrostatic thrust tilting-pad bearing (position 8) against the shaft collar (position 7) and furthermore against the test bearing.

Operating Conditions

Table 4 gives an overview on the main operating conditions of the test-rig related to this presented investigation.

Table 4 Operating conditions

Specific thrust load	0 ... 508 <i>psi</i>	(0 ... 3,5 <i>MPa</i>)
Shaft speed	0 ... 20,000 <i>rpm</i>	(0 ... 20'000 <i>1/min</i>)
Surface speed at mean diameter	0 ... 17,716 <i>fpm</i>	(0 ... 90 <i>m/s</i>)
Oil supply temperature	113 ... 131 °F	(45 ... 55 °C)
ISO viscosity class	ISO VG 32	
Oil supply flow	3.57 <i>gpm</i>	(13.5 <i>l/min</i>)
Inner axial bearing diameter	2.13"	(54 <i>mm</i>)
Outer axial bearing diameter	4.65"	(118 <i>mm</i>)
Mean axial bearing diameter	3.39"	(86 <i>mm</i>)

Instrumentation

- The test-rig bearing includes several transmitters to validate the calculation results: **Figure 3**:
 - Temperature probe MS1.3 at 75%/75% according (API 670); (at 75% of pad length from leading edge and 75% of pad width radially from inner axial diameter)
 - Temperature probe MS1.4 at 75%/50%
 - Temperature probe MS1.2 at 50%/50%
 - Temperature probe MS1.1 at 6.5%/75% (to measure leading edge temperature)
 - Distance from each temperature probe to Babbitt bond zone is 0.8 *mm* (0.0315") and its tolerance of +0.3 *mm* (0.0118") according (API 670)
- Standard thrust pad (pad II. to VI.):
 - Temperature probe MS n .1, ($n=2...6$ according nomenclature of the standard pads): 75%/75% according (API 670)
- Pocket temperature (MT1 and MT2) arranged on the spray bar before and after the main thrust pad
- Inner pad side flow (M11), which is located on an isolator at the side face of the main thrust pad to measure the temperature of the flow radially leaving the inner diameter of the pad – see flow $\dot{V}_{i,j}$ from **Figure 6**.
- Oil supply temperature (MZ1 and MZ2) located in the spray bar
- Oil drain temperature (TX i , $i=1...3$) located symmetrical (each 120 °) around the bearing center on an oil drainage plate
- Static thrust load (F)
- Turning speed of the shaft (N)
- Friction torque measurement (MPV)
- Transmitters within the hollow shaft provides:
 - Oil film thickness measurement (S1 and S4, both shift by 180° around the bearing center) positioned at a pitch diameter of \varnothing 3.2480" (or \varnothing 82,5 *mm*)
 - Thrust collar temperature (MJ)
- Oil system includes:
 - Tank temperature, supply temperature, return flow temperature, supply pressure

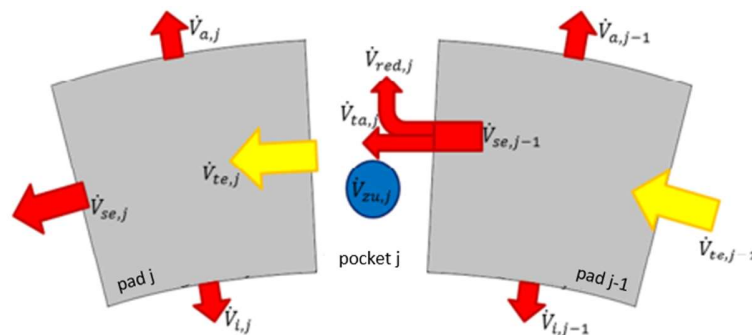


Figure 6 Flow distribution within the thrust bearing (Schwarze and Kraft, 2013)

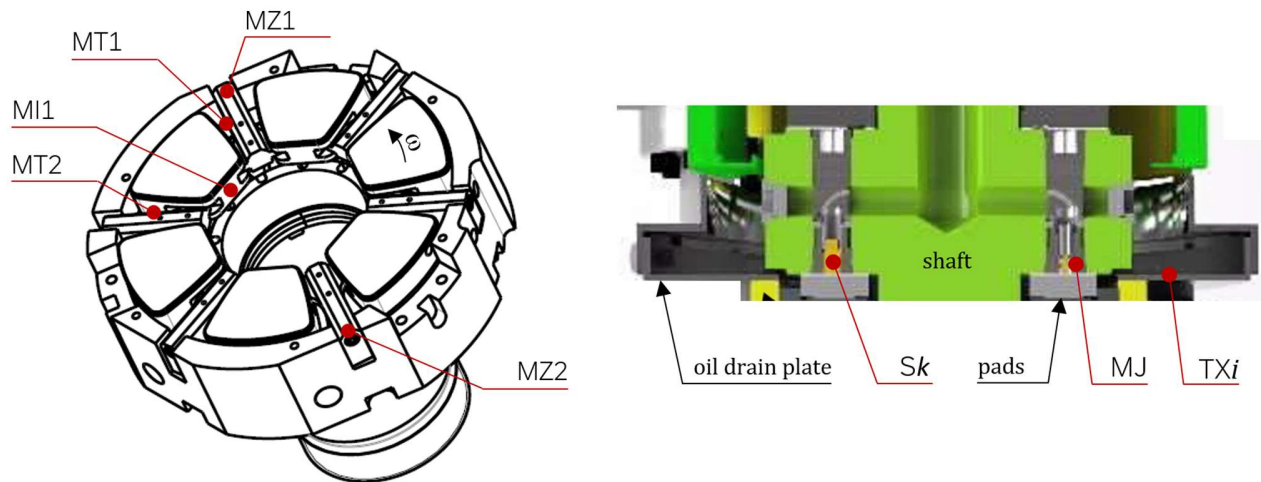


Figure 7 Measurement probes of the bearing (*left*) and shaft or housing (*right*)

Where:

- MI = Measurement probe of inner side flow
- MT = Measurement probe of pocket temperature
- MZ = Measurement probe of supply temperature
- S = Measurement probe of oil film thickness
- MJ = Measurement probe of thrust collar temperature
- TX = Measurement probe of oil drain temperature

Figure 7 shows the location of the different measurement probes. Please note, the right figure is just a schematic view and shows a flooded bearing. **Table 5** includes the measurement uncertainties on the different transmitters for information.

Table 5 Measurement uncertainties

Thrust load	$\pm 29 \text{ psi}$	$(\pm 0,2 \text{ MPa})$
Power loss, strain gauge	$\pm 0.174 \text{ hp}$	$(\pm 0,13 \text{ kW})$
Power loss, temperature	$\pm 1.303 \text{ hp}$	$(\pm 0,9715 \text{ kW})$
Oil supply flow	$\pm 0.07133 \text{ gpm}$	$(\pm 0,27 \text{ l/min})$
Oil supply pressure	0.25 %	
Oil supply temperature	$\pm 1.8 \text{ }^\circ\text{F}$	$(\pm 1 \text{ K})$
Thrust pad temperature	$\pm 1.8 \text{ }^\circ\text{F}$	$(\pm 1 \text{ K})$
Oil film thickness	2.7 %	

EXPERIMENT AND PREDICTION

Test Procedure

The first test series includes the reference support ring V1 and miscellaneous speeds, loads and oil conditions to check test-rig plausibility. The following test campaigns V1 to V4 include the different support rings and thus different misalignment – see **Table 3**. **Table 6** shows the test regime of each test campaign. Each speed increase includes a period of 5 minutes to balance potential transient temperature behavior before the different load steps (according to the load steps of **Table 6**) are applied. Each load increase also includes such a balancing time of 2.5 *min*. The balancing time results from a previous internal experimental plausibility test and obtains that there is no temperature overshoot.

Table 6 Test regime of each test campaign

Specific thrust load	73, 145, 290, 435, 508 <i>psi</i>	(0,5; 1; 2; 3; 3,5 <i>MPa</i>)
Turning Speed	0...17,500 <i>rpm</i>	(0...17'500 <i>rpm</i>)
Oil supply temperature	113, 131 <i>°F</i>	(45, 55 <i>°C</i>)
ISO viscosity class	ISO VG 32	
Oil supply flow	3.57 <i>gpm</i>	(13.5 <i>l/min</i>)

Figure 8 shows the transient temperature behavior due to load changes. The temperature measurements do not indicate a temperature overshoot after the load increases or decreases by factor 2. The authors therefore assume a steady-state approach for the test-rig.

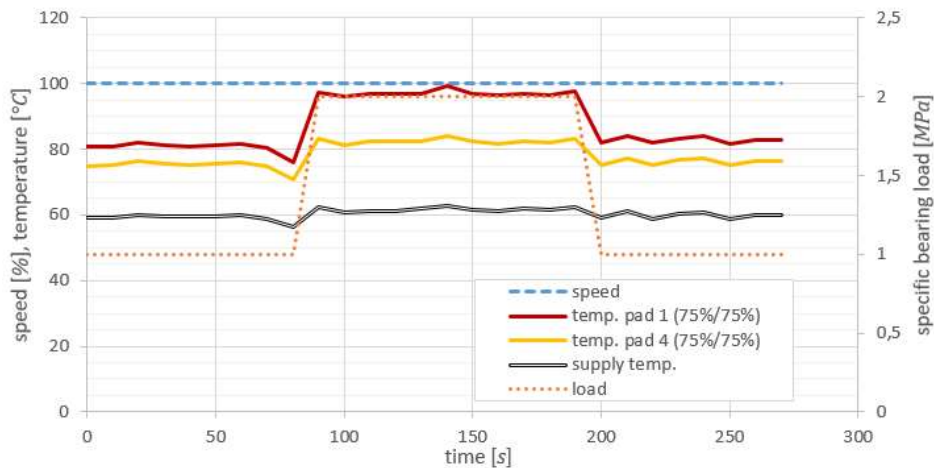


Figure 8 Transient test-rig behavior at 12,000 rpm and with misalignment ring V3

Test Campaign without Misalignment

First validation compares the calculation with the results of test campaign “V1”, which includes almost no misalignment to the support ring and thus induces a relative small bearing and collar misalignment only.

Figure 9 and **Figure 10** show the comparison of measured pad temperatures of pad I to pad VI instrumented as per (API 670) – with 75 % of pad length from leading edge and 75 % of pad width radially from inner axial diameter – and calculated temperatures at equal location at the pad. MS1.3 describes the temperature probe of the high-loaded pad I., MS2.1 to MS6.1 the corresponding temperature probes of the pads II. to IV., see chapter Instrumentation. The figure include a wide range of turning speed N and specific bearing load \bar{p} . It additionally include the oil supply temperature. The temperature spikes of the calculated temperatures relate to a changing oil supply temperature from the measurement, which is used as an input parameter for the calculation. The validation of the bearing calculation software shows a very good correlation of the measured temperatures at the different loads and speeds.

The spread on the measured pad temperatures itself relates to the residual pad misalignment, which exists due to the friction of the different contact elements such as the leveling links, spherical pivot of each thrust pad and contact to the housing. This effect is for example also described in Koosha (2020) and Glavatskih (2002).

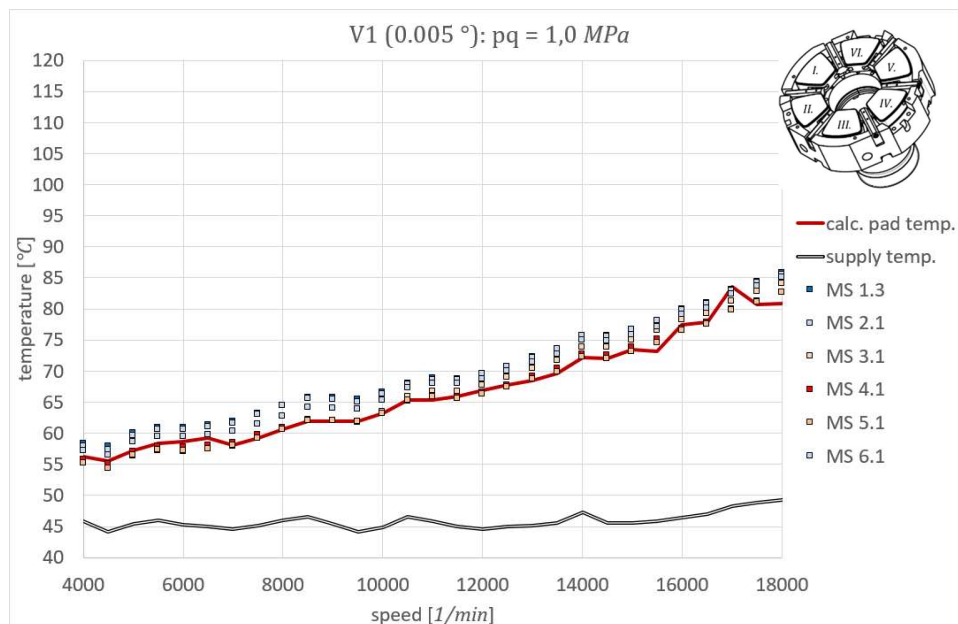


Figure 9 Comparison on measurement and calculation of the pad temperatures, test-campaign V1 at specific load of 1 MPa (145 psi) within speed variation and a supply temperature of 45 °C (113 °F)

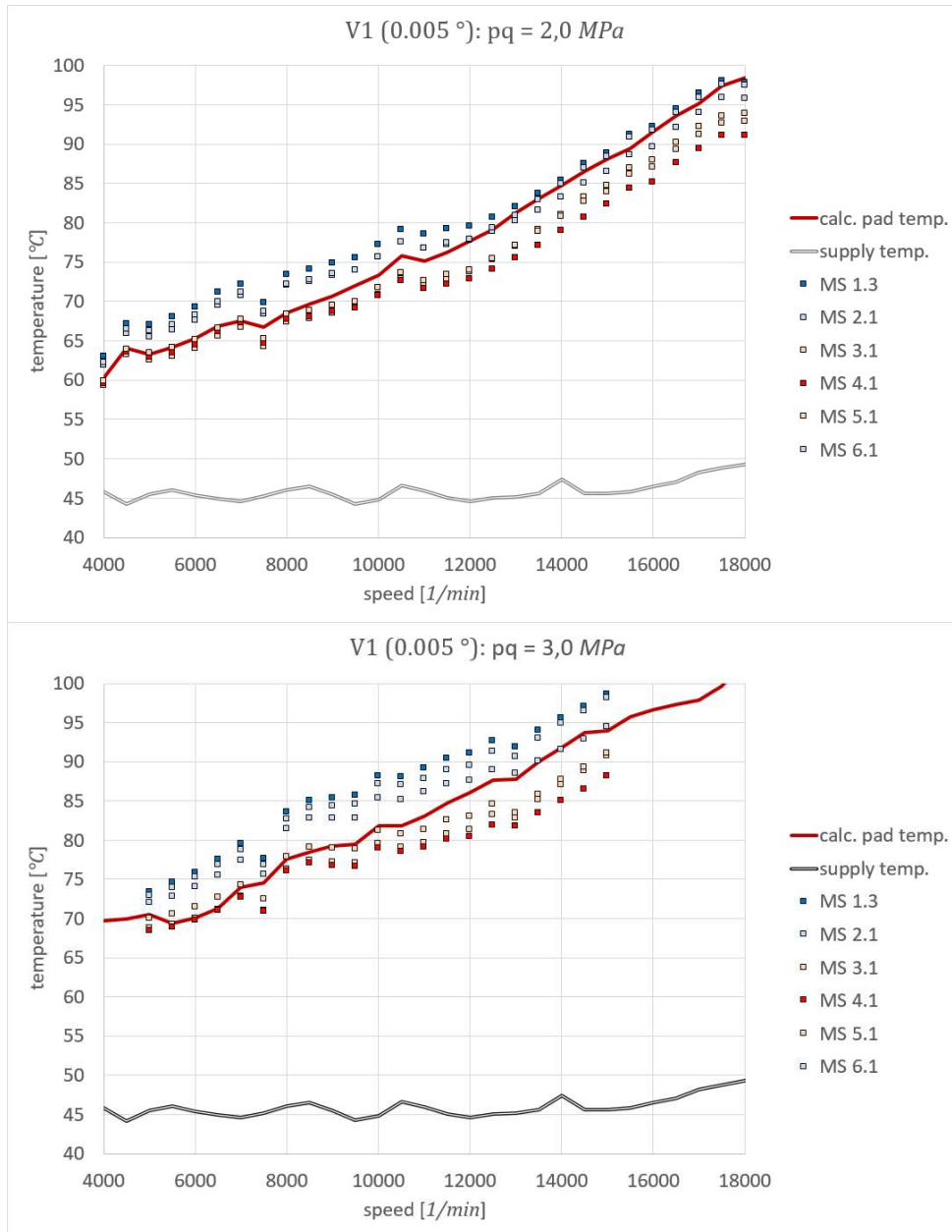


Figure 10 Comparison on measurement and calculation of the pad temperatures, test-campaign V1 at specific load of 2 and 3 MPa (290 and 435 psi) within speed variation and a supply temperature of 45 °C (113 °F)

Where;

- N = Turning speed in *rpm* (1/min)
- \bar{p} = Specific bearing load $\bar{p} = F / (B_{ax} \cdot L \cdot Z_{ax})$ in *psi* (MPa)
- B_{ax} = Pad width $B_{ax} = (D_o - D_i) / 2$ in inch (mm)
- L = Pad length: Arc length between leading and trailing edge at D_m in inch (mm)
- D_m = Mean axial diameter $D_m = (D_o + D_i) / 2$ in inch (mm)

Test Campaign under Misalignment

Figure 11 shows the residual pad misalignment depending on the initial bearing to collar misalignment. The initial (static) misalignment was machined into the bearing’s support ring, see **Figure 3**. The residual pad misalignment is measured by the transmitter of the oil film thickness (S1 and S4) and results from the axial distance between the pad surfaces of the pad with the nearest distance to the collar and the pad surface with the largest distance to the collar. According to the machined misalignment within the support ring and the arrangement of the tilting pads and its nomenclature, pad *I*. equals the nearest distances between the collar and bearing, pad *IV*. equals the largest distance. For a better handling, please note that the following residual pad misalignment values are converted from the position of the measurement transmitter of $\varnothing 3.2480''$ (or $\varnothing 82,5\text{ mm}$) to the outer axial bearing diameter $\varnothing 4.65''$ (or $\varnothing 118\text{ mm}$). The results show that the residual misalignment decreases while the thrust load increases. Besides the existence of the residual pad misalignment, which relates to the friction of the contact elements (leveling links, spherical pivot and housing), the measurements show that the leveling links almost equalizes the manufactured bearing to collar misalignment.

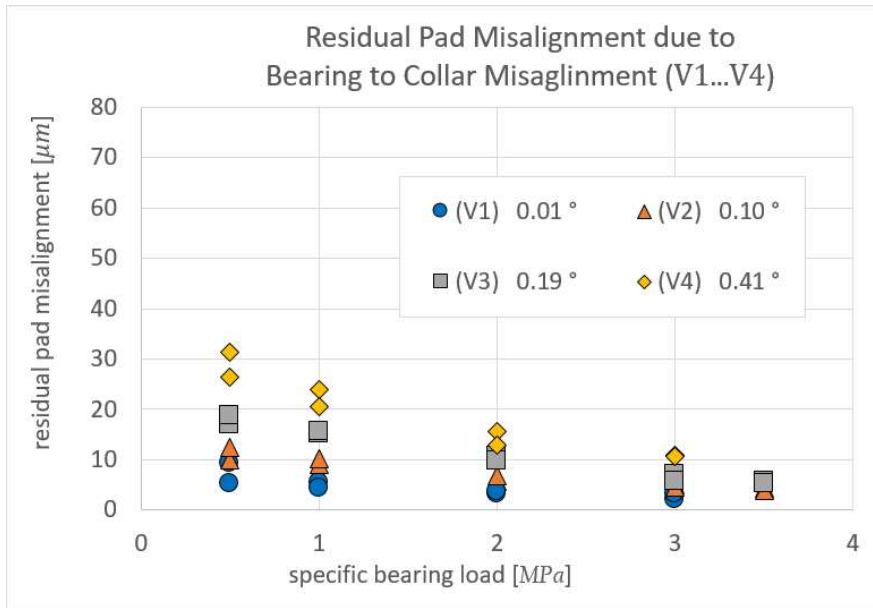


Figure 11 Measured residual pad misalignment for bearing to collar misalignment of $\alpha = 0.01...0.41^\circ$, supply temperature of $45...55^\circ\text{C}$ ($113...131^\circ\text{F}$), specific load from $73...508\text{ psi}$ ($0,5...3,5\text{ MPa}$)

Re-Calculation of the Measurements under Misalignment

The used bearing calculation software does currently not include a self-equalizing model. However, it includes the degree of freedom to include a constant angular bearing to collar misalignment. Thus, the following calculations include the difference of the maximum and minimum measured residual pad misalignment to re-calculate the bearing. **Figure 12** shows the measured and as a result the calculated oil film thickness. Similar to the measurement, the calculated minimum film thickness considers the position of the transmitter. The left figure of V2, which is equal to a misalignment of 0.095° , shows a very good match especially at the maximum and minimum value. However, the periodic course and its absolute values of the right figure of V3, which is equal to 0.188° , present some differences to the measurement.

This indicates the current calculation model is not sufficient to predict self-equalizing thrust tilting pad bearings under bearing to collar misalignment.

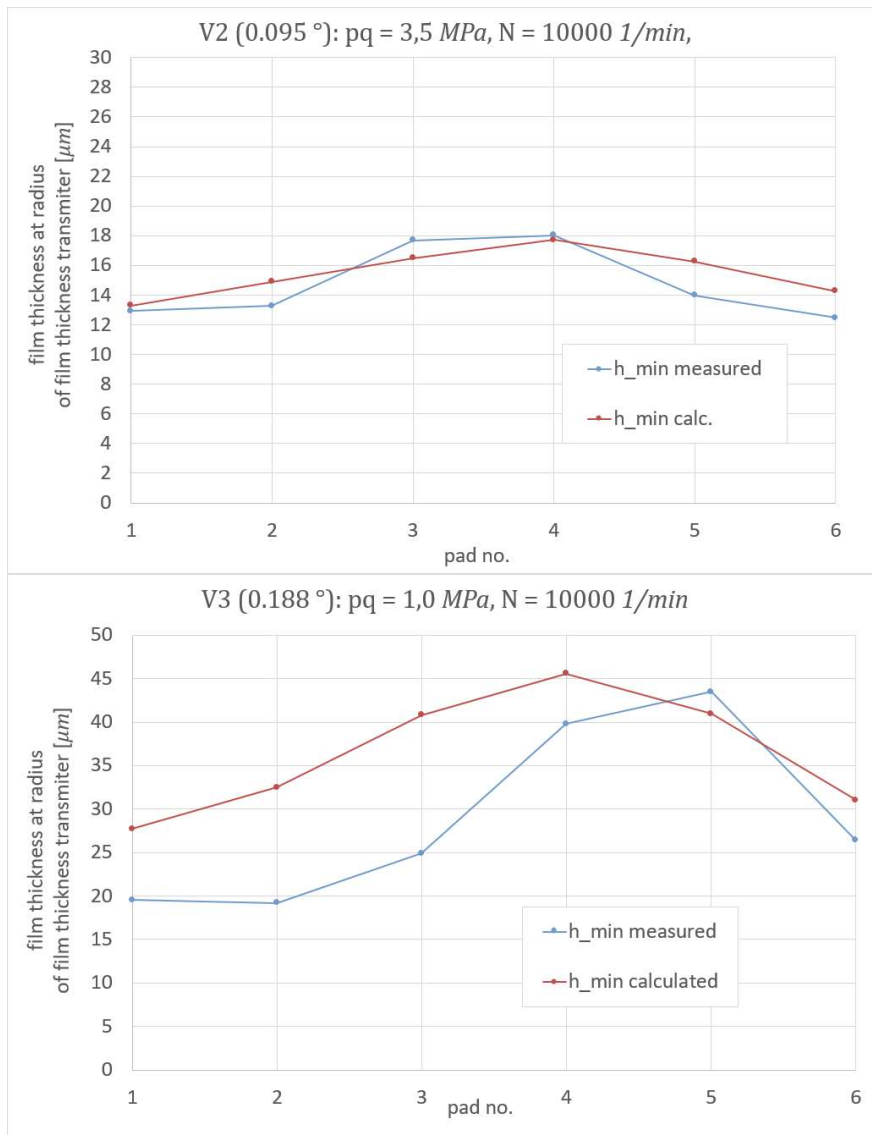


Figure 12 Measured and calculated oil film thickness in direction of rotation from pad I to pad VI (the upper figure shows support ring V2, the lower figure support ring V3)

Figure 13 shows the calculated and measured temperature of pad I. and IV. of support ring V3. The discrepancy on the temperature difference between both pads (or from the residual pad misalignment) shows an asymmetrical pattern and the values do not match.

V3 (0.188 °): $T_{EN} = 45 \text{ °C}$, $p = 3,0 \text{ MPa}$
 residual pad misalignment according
 oil film thickness measurement of 0,006 mm

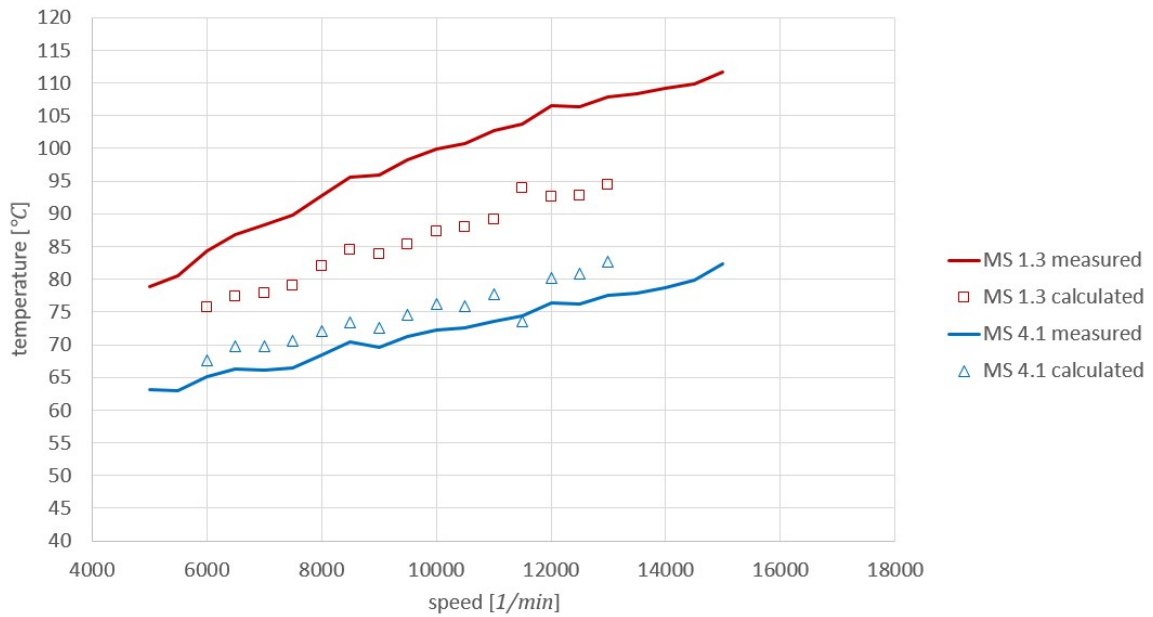


Figure 13 Comparison of measured and calculated pad temperatures of opposite arranged pad *I*. (temperature probe MS 1.3) and pad *IV*. (temperature probe MS 4.1) under misalignment of support ring V3. Calculation includes a bearing to collar misalignment according measurement.

Compared to the previous calculations, the following calculations include an iteration of the user-defined misalignment until the temperature distribution matches between measurement and calculation results. **Figure 14** shows the result on the pad temperatures of (the opposite arranged) pads *I*. and *IV*. at resulting minimum and maximum oil film thickness according to the described iteration.

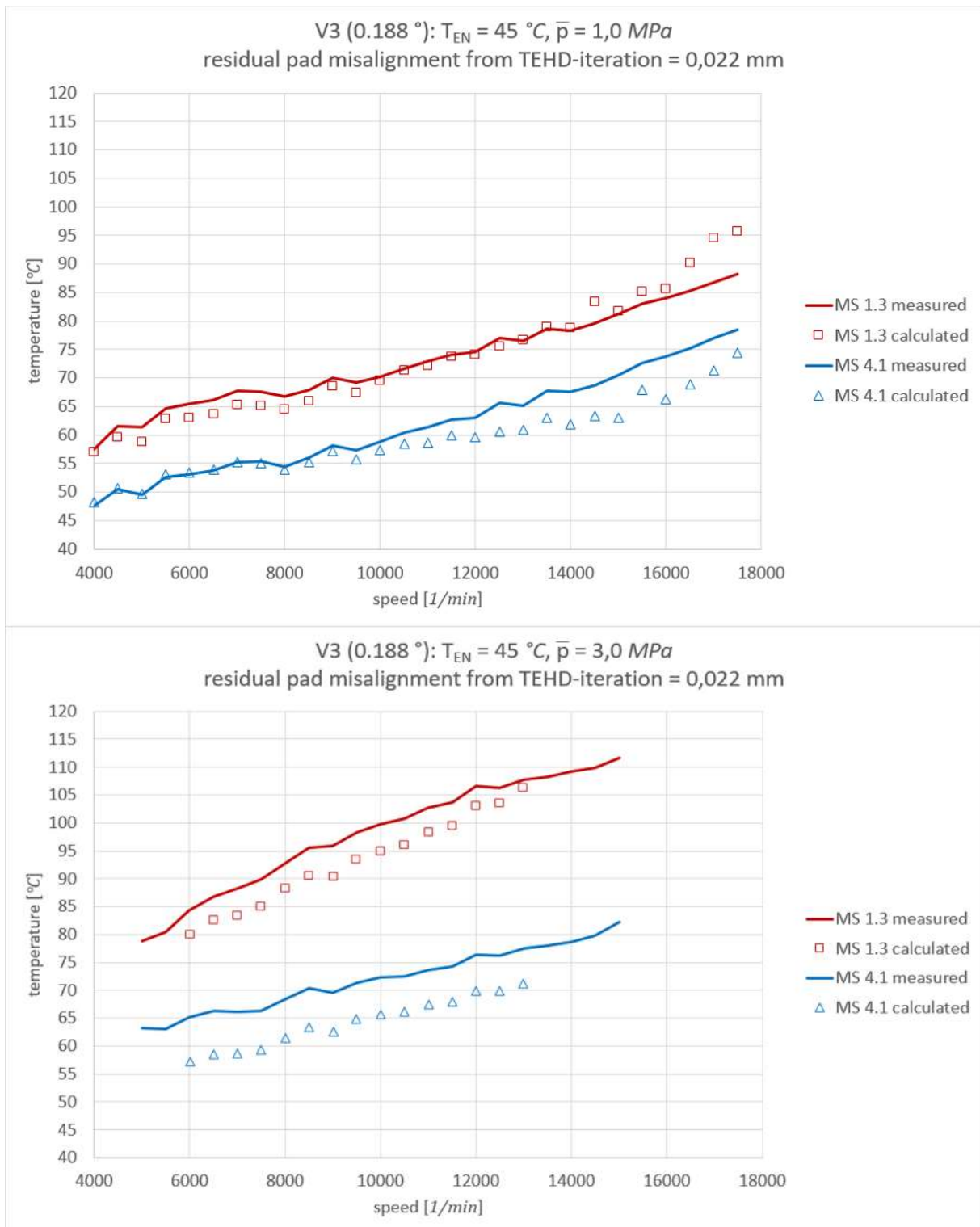


Figure 14 Comparison of measured and calculated pad temperatures of opposite arranged pad I. (temperature probe MS 1.3) and pad IV. (temperature probe MS 4.1) under misalignment of support ring V3. Calculation input of bearing to collar misalignment according user-iteration which fits best to measured pad temperatures.

Table 7 Calculated and measured residual pad misalignment of support ring V3

specific bearing load <i>psi (MPa)</i>	measured residual pad misalignment (Δ pad I to IV) <i>in (mm)</i>	calculated residual pad misalignment (Δ pad I to IV) <i>in (mm)</i>
145 (1,0)	0,00067 (0,017)	0,00086 (0,022)
435 (3,0)	0,00024 (0,006)	0,00086 (0,022)

Table 7 shows the residual pad misalignment between pad I. and IV. as a result of the previously described iteration procedure to achieve the optimal match between measured and calculated temperature distribution. It considers support ring V3, which equals a misalignment of 0.188 °. Both, the measured and calculated oil film thickness matches relative good at low loads of 1 MPa. However, the values are very different for higher loads. The calculated film thickness does not decrease at higher loads, which is not plausible – see also the prediction of Koosha (2020). The applied method to re-calculate the residual pad misalignment is therefore not sufficient.

OUTLOOK ON CALCULATING SELF-EQUALIZED THRUST BEARINGS

This paper presents data on the residual misalignment of the thrust tilting pads due to the misalignment between the bearing and collar. The finding of the residual pad misalignment is according to the description of Glavatskih (2002) and Koosha (2020). However – and as discussed previously – there is a discrepancy on the value of the residual pad misalignment which results from the comparison of the film thickness measurements and the results the temperature measurements implies. The difference may result due to errors in the measuring apparatus or for example due to the positioning inaccuracy caused by the relatively large manufacturing clearances which are required to permit a very large bearing to collar misalignment of 0.412 °.

To better understand the reaction of the self-equalized bearing, the following outlook will present a model to calculate the residual pad misalignment and to show further developments.

Flow Chart

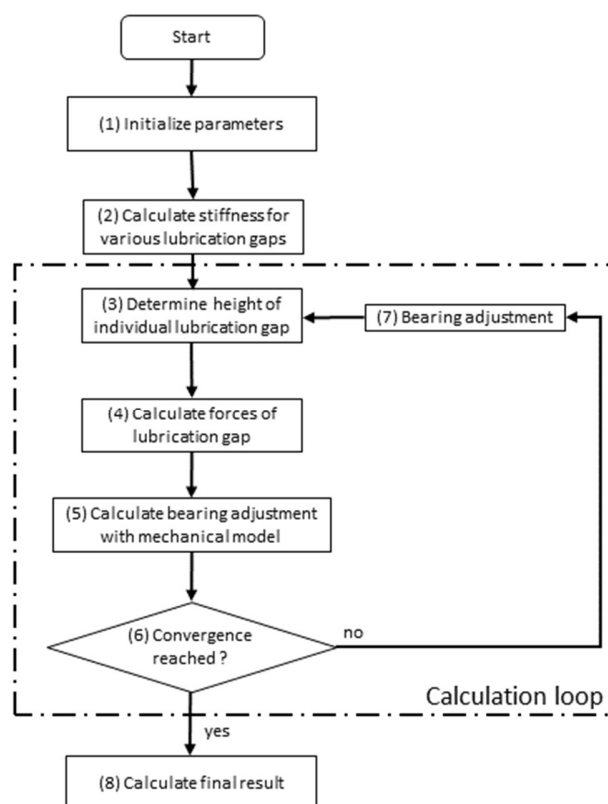


Figure 15 Flow-chart of the mechanical model (FEA-TEHD interface)

Figure 15 shows the flow chart of the mechanical model. The mechanical model was developed to link a FEA software and a thermo-elastic hydrodynamic software for fluid film bearings.

After the process has started, various parameters concerning the bearing and the collar including its misalignment are initialized (1). The data is then used to calculate the stiffness of the lubrication gap for each individual pad and for several heights of the gap (2). The bearing adjustment and the collar misalignment is then used to determine the height of the lubrication gap of each pad (3). Resulting from these heights the individual force of the gap is derived (4) from the stiffness matrix obtained in step (2). Taking these forces into account the mechanical model of the equalization mechanism is used to evaluate the systems reaction to the forces resulting in the movement of the equalizing elements (5). A convergence is then reached, if no further adjustment of the bearing is implied by the mechanical model (6). Otherwise the height of the bearing pads is adjusted (7) according to the results from step (5) and input into step (3). After the convergence is reached the adjusted bearing is used to determine the remaining data of the given operational point using the TEHD-Model (8).

Mechanical Model of the self-equalizing mechanism

The mechanical model calculates the reaction of the self-equalizing mechanism from the uneven load distribution of the different pads due to the misalignment introduced. The current model uses a FEA software for the calculation of the mechanism (steps 3 to 7 in Fig. 16).

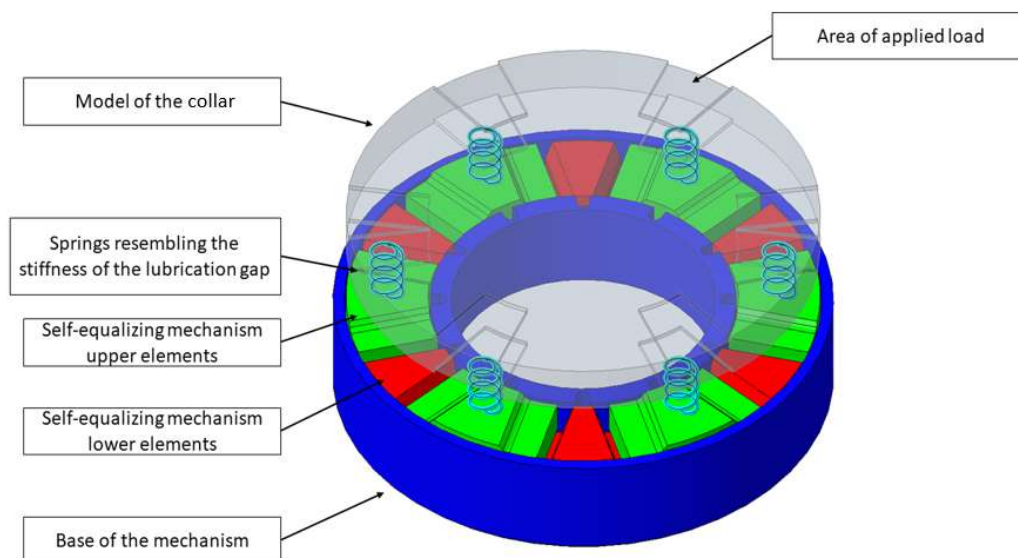


Figure 16 Bearing model for calculating self-equalized tilting pad thrust bearings

The areas of the applied load correspond with the location of the (green printed) upper leveling links. The springs represent the reaction of each lubrication gap due to its change of the leveling link displacement. On the one hand it damps the reaction of the mechanical system with an unbalanced load distribution, on the other hand it leads to a load penalty of pads with nearly no load unbalance. The stiffness of these springs derives from calculations using an elasto-mechanical model of the bearing.

The (blue printed) “base” (or support ring) of the mechanism includes fixed boundary conditions. All friction contacts of the leveling links and its guiding pins include a friction coefficient of $\mu = 0.02$, which represents a typical friction of lubricated steel.

Modifications of the TEHD software

To perform the previous discussed steps (2) and (8) of the flow chart shown in **Figure 15**, the used TEHD software required to be modified and now includes following adaptations:

- step (2): determine the stiffness of each lubrication gap for given conditions, this is used to generate the stiffness matrix of the lubrication gap
- step (8): calculate the residual misalignment resulting from the misalignment between bearing and collar and the leveling of the bearing and uses this to obtain the bearing reaction

Results of the bearing simulation

Figure 17 shows predicted residual pad misalignment of the bearing according to the developed model and the measurements from the test-rig. It shows that the calculated residual pad misalignment follows the expectation of Glavatskih (2002) and Koosha (2020) and decreases while the specific bearing load increases.

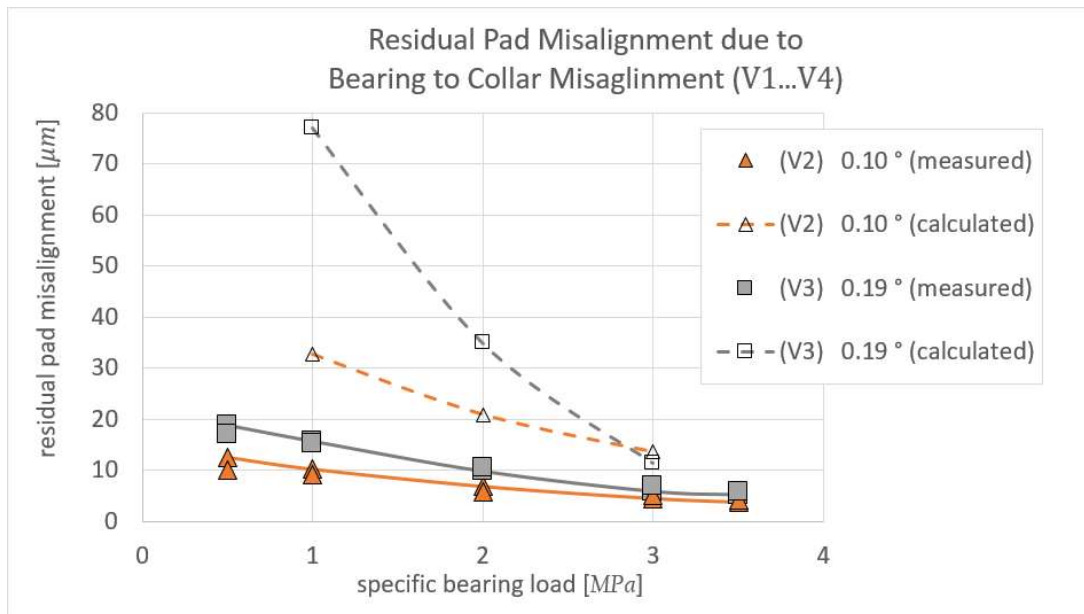


Figure 17 Measured and calculated residual pad misalignment for bearing to collar misalignment of $\alpha = 0.01...0.41^\circ$, specific load from 72...507 *psi* (0,5...3,5 *MPa*)

However, compared to the measurement the calculation shows high discrepancies on the absolute value. The calculation is two to five times higher than the measurement. This may be due to some simplifications within the modelling:

- The friction between all moving parts of the mechanical model is estimated to be constant of $\mu = 0.02$
- The Model does not distinguish between resting and gliding friction
- The contacts between the moving parts do not consider Hertzian contact areas.
- The misalignment acts exactly through the spherical support of pad *I.* and *IV.* and does not consider distortion.

Outlook on software development

The presented prediction of self-equalizing thrust bearings still shows discrepancies especially on the absolute values. From the authors prospective, the following points are recommended to be further development:

- Refinement of the current pad deformation algorithm
- Replacement of the current model by an analytical model, including more boundary conditions
- Research on the friction algorithm to determine the friction of the leveling links
- Adding Hertzian contacts for the elements contacting each other
- Implementing elastic deformation of the elements in the mechanism

CONCLUSION

This paper presents measurements, re-calculation and prediction of self-equalizing thrust tilting-pad bearings at various speeds, loads and bearing to collar misalignments. It shows, that self-equalizing mechanisms can level very high misalignments. The specific test set-up includes a maximum misalignment of 0.412° . The paper presents measurements on the residual pad misalignment due to friction of the contacts between the leveling links and the housing or tilting-pad and its resulting spread on the pad temperatures. Therefore, the measurements confirm the prediction of Koosha (2020), that the residual pad misalignment of high loaded applications can be neglected.

The validation of the used thermo-elastic hydrodynamic software according to the presented measurements without applying bearing to collar misalignment shows very good results. Additionally, the re-calculation by incorporating the measured residual pad misalignment as bearing to collar misalignment shows sufficient results for very low loads, too. However, the qualitative progression under increased load shows discrepancies.

To predict self-equalized thrust bearings, the paper presents the development of a mechanical model based on iterations between a FEA software and thermo-elastic hydrodynamic software. To achieve this, some adaptations to the used TEHD software are implemented, for example to individually determine the stiffness of each pad. The qualitative progression of the results meet the expectation, but the absolute values still show some discrepancies. For higher loads, the predicted residual pad misalignment is about two times higher than the expectation and for lower loads up to five times.

As an outlook, the authors present some recommendations, which might be further investigated to receive a more accurate prediction. The current mechanical model for example includes a constant friction for all contacts. Besides that, one of the authors will further develop the bearing calculation software to receive sufficient calculation results on self-equalizing thrust bearings.

NOMENCLATURE

B_{ax}	= Pad width $B = (D_o - D_i)/2$
D_i	= Inner axial bearing diameter
D_m	= Mean axial diameter $D_m = (D_o + D_i)/2$
D_o	= Outer axial bearing diameter
f_r	= Oil refreshing factor in the pockets between the pads
N	= Turning speed
P	= Power
\bar{p}	= Specific bearing load $\bar{p} = F/(B \cdot L \cdot Z)$
Q_{ax}	= Axial bearing oil flow
Δy	= height difference at the outer axial diameter
Z_{ax}	= Thrust pad quantity
α	= angle of bearing to collar misalignment resulting from the manufactured height difference Δy
TEHD	= Thermo-elasto hydrodynamic deformations

REFERENCES

- ANSYS, 2020 R1, CAE Software, ANSYS Inc.
- API 670, 5th edition, 2014, „Machinery Protection Systems“, *American Petroleum Institute*
- Bavassano, F., Mantero, M., Traverso, R., Livermore-Hardy, R., Blair, B., 2017, „A System Integration Approach for Heavy-Duty Gas Turbine Upgrades Using Improved Rotor Thrust Predictions and Application of Advanced Thrust Bearing Designs“, *ASME Turbo Expo 2017: Turbomachinery Technical Conference and Exposition*
- Capitao, J. W., 1976 „Performance Characteristics of Tilting Pad Thrust Bearings at High Operating Speeds“, *Journal of Lubrication Technology*, Jg. 98, No. 1, S. 81–88
- Capitao, J. W., Gregory, R. S., Whitford, R. P., 1976, „Effects of High-Operating Speeds on Tilting Pad Thrust Bearing Performance“, *Journal of Lubrication Technology*, Jg. 98, No. 1, S. 73–79
- Elrod, H., 1981, „A cavitation Algorithm“, *Transactions of the ASME*, Vol. 103
- Gardner, W., 1985, „Performance characteristics of two tilting pad thrust bearing designs“, *Proceedings JSLE International Tribology Conference*, S. 61–66
- Glavatskih, S. B., 2002, „Laboratory Research Facility for Testing Hydrodynamic Thrust Bearings“, *Proceedings of the Institution of Mechanical Engineers Vol. 216, Part J: Journal of Engineering Tribology*
- Glienecke, J., Lindloff, K., Medhioub, M., 1994, „Hochbelastete Axialgleitlager“, *BMW/AiF*, Nr. 8995
- Gokaltun, S., DeCamillo, S., 2019, “Computational Analysis of the Equalization Behavior of Thrust Bearings With Regular and Modified Leveling Plates”, *ASME Turbo Expo 2019*
- He, M., Byrne, J., 2018, Fundamentals of Fluid Film Thrust Bearing Operation and Modeling”, *Turbomachinery Laboratory, Texas A&M Engineering Experiment Station*
- Heshmat, H., Pinkus, O., 1986, „Mixing Inlet Temperatures in Hydrodynamic Bearings“, *Journal of Tribology*, Jg. 108, No. 2, page 231–244.

- Iordanoff, I., Stefan, P., Boudet, R., Poirier, D., 1995, „Dynamic Analysis of a Thrust Bearing—Effect of Misalignment and Load“, *Proceedings of the Institution of Mechanical Engineers, Part J: Journal of Engineering Tribology*, Jg. 209, Nr. 3, S. 189–194
- Koosha, R., 2020, “a thermo-elasto-hydrodynamic (TEHD) computational analysis for the force performance of self-equalizing tilting pad thrust bearings”, *dissertation at Texas A&M University*.
- Koosha R., San Andrés, L., 2020, „A Computational Model for the Analysis of the Static Forced Performance of Self-Equalizing Tilting Pad Thrust Bearings“, *Journal of Engineering for Gas Turbines and Power*, Jg. 142, Nr. 10
- Monkova, K., Urban, M., Monka, P., Moravka, S., Božić, Ž., 2021, „Design of the levers at the development of new self-equalizing thrust bearings“, *Procedia Structural Integrity* 31, S. 92–97
- Schwarze, H., Kraft, C., 2013, „Verbesserte Axialgleitlagerberechnung“, *Forschungsvereinigung Verbrennungskraftmaschinen (FVV)*, Nr. 1019